Applications of Electromagnetic Fields and PDMS-Based Microfluidic Structures for the Entrapment and Rotation of Cells

Thomas S. White[a], Dr. Qin Hu[b], and Dr. Tolga Kaya[c]

School of Engineering and Technology

Central Michigan University, Mount Pleasant, Michigan, 48859

E-Mail: [a]white1ts@cmich.edu; [b]hu1q@cmich.edu; [c]kaya2t@cmich.edu

Abstract: The amount of time a physician has to respond to a medical emergency, such as major injuries or severe illnesses, can be crucial to a patient's recovery. Any tool that gives medical professionals a faster method of detecting diseases could increase their patients' chances. Entrapment and electro-rotation (ROT) of cells is one method being explored to help realize this aim. The premise is that cells of different sizes resonate to different electrical frequencies. This means that larger cells can be separated from smaller cells in an electromagnetic field. The literature indicates this to be a promising prospect. We present a device design that will be fabricated through photolithography processes, metal deposition, and PDMS for creating microfluidic channels. These devices are intended to function by generating an electromagnetic field via the introduction of four different electrical signals phased 90° to one another. The goal is to induce the cells to gather in the center of the e-field via electrodes also positioned 90° to one another. According to the literature, voltages ranged from 0.4V to 0.6kV in various ROT experiments. Calculations indicated a 5V potential best fits our current design's needs. Initial tests will be conducted using polystyrene micro-beads to simulate the responses of spherical cells. Once this process can be replicated reliably, testing will move forward to living specimens such as algae or malignant cells; this could include the eventual incorporation of nanoparticles like silicon or iron-oxide to observe how they affect cell responses to electromagnetic fields.

I. Introduction

It is important for doctors and other health professionals to have the best tools at their disposal to help their patients. One avenue being explored is the application of electric fields for the purposes of entrapping and rotating cells[1-14]. The premise of this research is that cells of different sizes resonate to different electrical frequencies[1-14]. Dielectrophoresis can induce dipoles in cells. Induced dipoles can be used to draw the specimens from one side of a container to the other through the application of electrical potentials[6, 9-11]. With time and refinement, this research could lead to devices that quickly detect illnesses--such as cancer--by separating the diseased cells from the healthy ones—giving medical professionals more time to act [1-11]. Such devices also offer a benefit of low power consumption in addition to their small size, portability and accuracy. However, this research is still relatively in its early stages. Fully functional devices might be still be several years away at least.

Like other forms of experimental research, finding the most reliable methods and designs are serious challenges. For example, both stationary and moving electromagnetic fields have been evaluated to test their viability[1-5, 7, 8]. Some designs incorporated a top and bottom electrode system, while others employed a series of magnetic coils placed around the sample, and yet others only used a bottom electrode for generating a moving field[2, 3, 6]. In the case of cancer cells that spread through the blood, locating and separating malignant cells can be difficult when facing a concentration of a few cancerous cells per million healthy cells[3]. Dielectrophoresis has been used effectively for separating and moving cells as desired[1-5]. Once the cells are captured, a reliable means of stimulating rotation must be implemented. This can be accomplished by employing 4 electrical signal phases at 90 degree angles to one another. The intention is to create an electric field that will push the entrapped cells into the center to encourage rotation. In some experiments, researchers introduced nano- and micro-particles such as iron oxide, gold and silicon to enhance effectiveness of the electromagnetic field[2, 3] Other experiments revealed that such particles contributed to cell death by rupturing the cell walls, despite temporarily enhancing rotational behavior; the gold and silicon particles appeared to cause cell death most often[2]. In another series of trials, it was found that the e-field proved lethal to cells while the iron-oxide particles actually helped prolong cell life during tests[3]. Regardless of the methodology, the main point is to entrap and rotate the samples so that their behavior can be observed, recorded and analyzed.
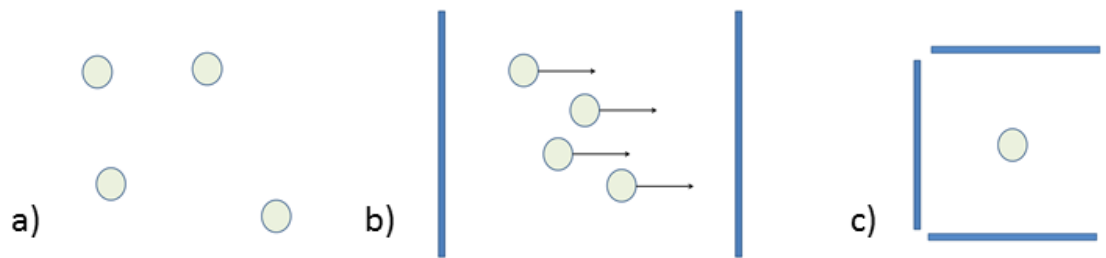
Figure 1: A simulated image of the suggested process for cells a) without the application of the electric field, b) with the dielectrophoresis to maneuver cells into place, c) with all four phases active to create the e-field to entrap and rotate a cell[1, 3].

Fig. 1a-c illustrates how the cells would ideally respond to a proper electric field. They would transition from a state of separation to closely grouping together at the center of the field. Dielectrophoresis would move the samples into place so as to trap them in the full electromagnetic field. The center of e-field is where rotation occurs. The basic concept for the device can be seen in Fig.2. The proposed device will contain copper electrodes on insulating glass substrates. PDMS is intended form the chamber walls and the microfluidic channels to direct the cells as desired. This is meant to be a simple, but effective design.
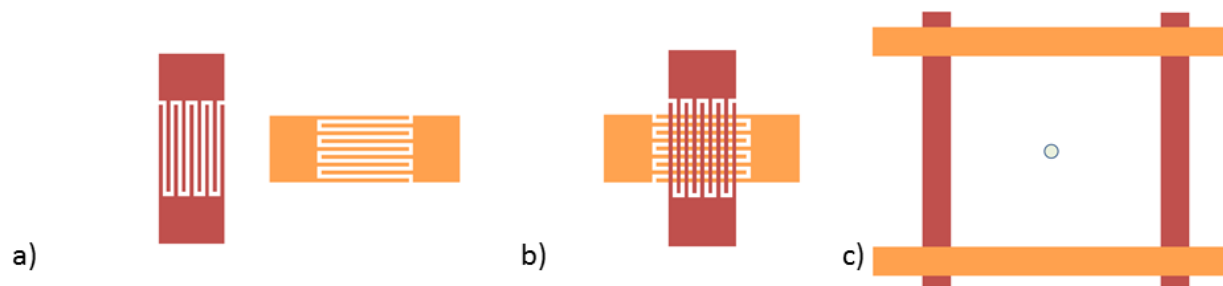

Figure 2: The basic premise for the device can be seen in a) the two separated electrodes with the inter-laced capacitance plates, b) the device as it would be constructed with the two electrodes overlapping for creating the e-field, and c) a close up of the inter-locked capacitance plates where the cells would be entrapped when the electrical frequencies are in phase. In all three images the electrodes were colored differently to demonstrate that they are not fused together.

Fig. 3-5 demonstrate the configuration and ideal performance of the four electrodes. These were derived from simulations run in COMSOL Multi-physics. The simulated sinusoidal voltage applied to each electrode has a magnitude of 5V at a frequency of 100Hz. This frequency is intended to first trapping the cell in the electrode chamber before attempting to rotate it. The voltages on the two opposing electrodes have a phase shift of 90 degrees. Once the cell is in

position, an electrical potential will be applied across the remaining electrodes to complete the e-field and initiate cell rotation. A 3-D Laplace equation was solved with Dirichlet boundary conditions to obtain voltage distribution within the chamber[4].This is a form of differential equation often used for calculating limitations and boundaries. In this case, it was used to calculate a functional dispersion of the electric field between electrodes. Formula 1 represents this relationship. The root-mean-square (RMS) voltage distribution for the middle plane in the z direction (z = 0) at T = 10ms is shown in Fig .4. It is a projected snapshot of how the field would behave at 10ms. The center of the e-field has a voltage of zero which allows cells to rotate as the electric forces only act on them from around the center.

Once the biological samples are in the chamber, they will sense the dielectrophoretic force (DEP). It is a spatially non-uniform electric field. This field will help to induce polarization in cells. The dielectrophoretic force acting on a spherical cell can be found from the following equation:

$$F_{DEP} = \frac{3}{2}v_{cell}\varepsilon_{med}\,\text{Re}[K_{CM}^{*}(f)]\nabla E^2 \qquad . \tag{1}$$

Formula 1 basically shows a direct, proportional relationship between DEP and the volume of the cell, v_{cell}, the electrical permittivity of the suspending medium, ε_{med}, and E the "root-mean-square (RMS)" value of the external electrical field. $K_{CM,\alpha}^{*}$ represents the complex Clausius-Mossotti factor of this equation while Re is its real counterpart[4].

Fig. 3 shows a contour map of the dielectrophoresis force (DEP) factor at the center of the plane (Z = 0). According to our simulations the high DEP force on the edges should push cells to the center. Once there the zero DEP force can keep cells trapped as long as the external voltages are applied. This is made possible by the direct relationship between the e-field and the DEP illustrated in Formula 1.
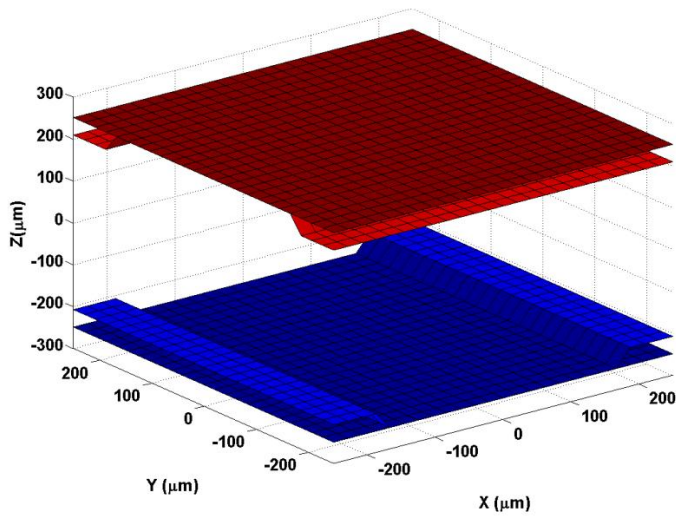
Figure 3: Electrode Configuration with two electrodes on top and bottom respectively. The Chamber has a dimension of 508µm(L)×508µm(W)×500µm(H).

Fig. 4-5 help to further demonstrate the behavior or the electromagnetic fields. In Fig. 4, we see the voltages as they are applied from the 4 phases. Notice how it drops to a point at zero on the central z-plane (Z=0). A very similar behavior is demonstrated with regards to the force factor on the x- and y- planes of the electrodes (a 400 µm by 400 µm area) in Fig. 5. In the center of the square area of the field, the force activity is zero.
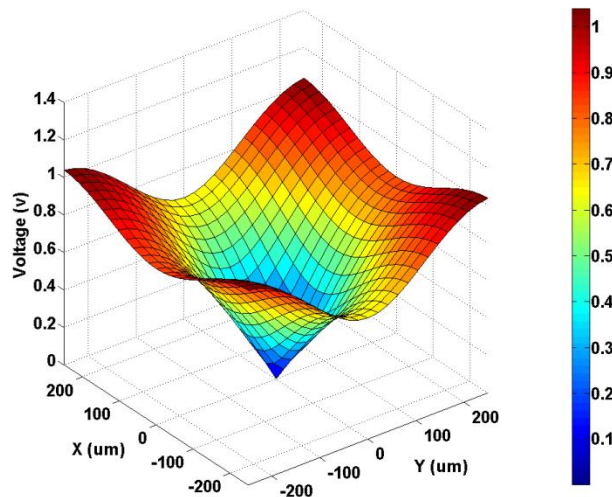

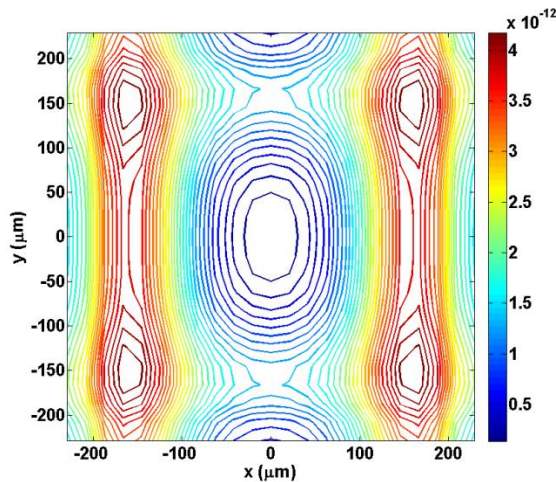Figure 4: Voltage (RMS) distribution on the z = 0 plane at time T = 10ms.

Figure 5: Dielectrophoresis force factor on the z-plane, where z = 0 at T = 10ms.

Observing and recording rotational behavior can be the next challenge to overcome. It often requires extra measures to enhance sample visibility[1-8]. Laser Induced Fluorescence (LIF) is one technique that enhances the visibility of cell movement[3, 4, 10]. Graphene-oxide has shown a capacity for fluorescence when exposed to certain light wavelengths[15, 16]. Computer algorithms have also proven useful for recording cell rotation[7, 8]. They generated plots based on frame-by-frame picture data gathered during tests; the outlines of the cells were traced in each frame to make their movement more distinguishable[7, 8].

In addition to being able to observe cell behavior, there is the practical matter of properly guiding the test samples into an electrode chamber. Microfluidic channels are an efficient means of doing this. One method for creating microscopic channels is to chemically etch them onto a glass substrate[10, 11, 17]. A simpler method makes use of Polydimethylsiloxane (PDMS)—a silicone similar to rubber[8]. The latter method is quicker and also does not require the use of dangerous etchants like Hydrofluoric Acid (HF). PDMS can be easily molded on a silicon wafer with a UV sensitive masking agent such as SU-8. PDMS offers the opportunity to efficiently create both the desired channels and the electrode chamber walls at the same time[18]. Fig. 6 helps to demonstrate the basic idea for using the PDMS to produce a mold. Initial tests for the device made use of a special tape approximately a 100 nm thick. The micro-beads have a diameter of 14.7μm so, we decided that 50μm by 100μm would allow sufficient room to direct the micro-beads through the channels. The PDMS will be used at a later time in this project once the mold fabrication process yields sufficient results.
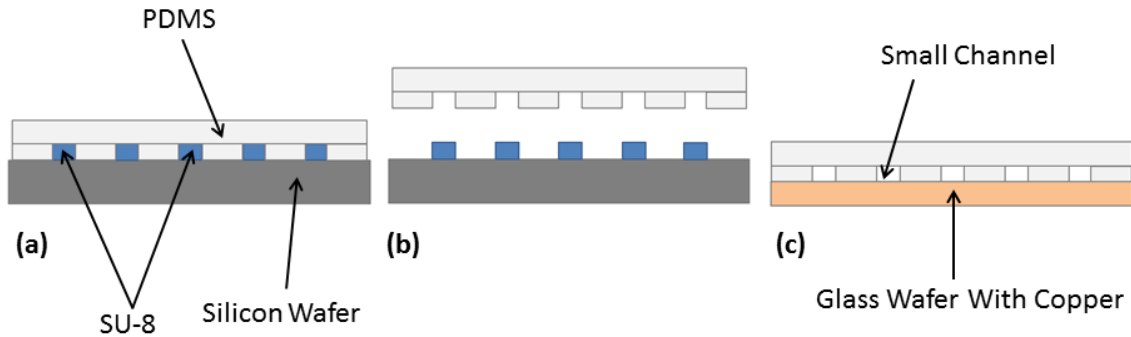
Figure 6: The PDMS process a) as it is molded with SU-8 on a silicon wafer, b) after it has cured and can be separated from the mold, c) applied to the glass slide with the copper components. The small channels will be ideal for guiding the microbeads and cells to the electrode chamber.

Currently, the entire design and fabrication processes for this device have been carried out in Kaya Lab on Central Michigan University's (CMU) campus. Programs such as AutoCAD and COMSOL Multi-physics will continue to be crucial for designing and simulating the performance of possible designs. The electrodes have already been fabricated by depositing copper onto a glass slide and then shaping it through photolithography and chemical etching. The PDMS component will be attached between the electrodes. This will allow for the electro-rotation to be observed from above via a microscope or camera. The PDMS structure will also provide a stable, even structure to support the two glass slide sections containing the electrodes. An added benefit of this method is that the chamber walls could be removed and reapplied as needed during evaluations of the devices. The testing itself will include experimentation with various electrical frequencies to isolate the ones that most effectively separate cells.

The first step in this research is to successfully capture and rotate an individual cell. Once this is accomplished, experimentation can move onto deeper analysis of frequencies that yield the desired responses from cells of various sizes and shapes. This will also allow for later comparison with earlier calculations to evaluate their accuracy. Future goals include examining cells taken from various tissue samples, such as blood and tumor sites. The ultimate aim of this work is to contribute to the growing body of knowledge in the hopes of providing medical professionals and their patients a better means of diagnosing disease.

II. Design

Fig.7 shows an earlier prototype of this design. As can be seen the top and bottom slides are crossed over one another to be conducive for generating the desired electromagnetic field. Silver paint was used to fasten the wires to the electrodes. These wires were then connected to a function generator that created the needed potentials.
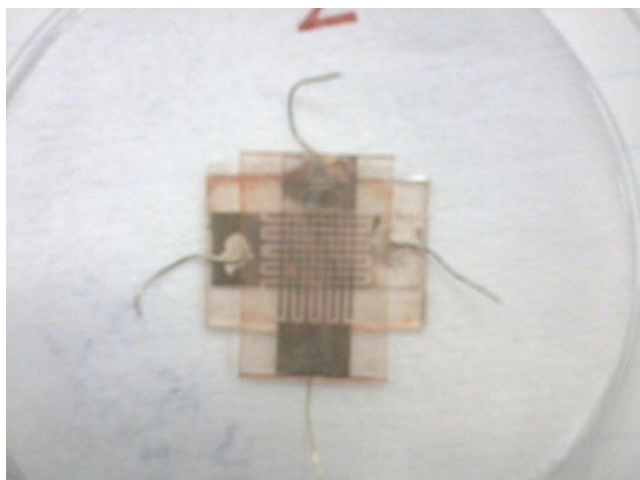
Figure 7: An early version of the proposed device. The wires on the electrodes were fastened with silver paint. The electrodes were positioned facing one another, crossed, to attempt to create the desired electromagnetic field. Tape held the electrodes in place during initial trials.

As there were only two lines coming out of the generator, the lines were each split into two. Each additional line was connected to an inverter to help create the needed frequencies for the signal phases. The initial phase and voltage parameters were similar to the projections provided in Fig.3-5.

Several trials with this early prototype failed to show any response from biological samples placed within the chamber. It was suspected, at the time, that inappropriate cell samples were used. Osteoblasts were used for the initial tests. They tend to cling to surfaces so that they can create bone in a process called scaffolding [19]. Swishing the container occasionally helped prevent the osteoblasts from settling long enough to begin scaffolding, but they still didn't appear to respond well. We decided to try polystyrene microbeads because they behave similarly to cells, yet they don't expire. Another possible cause of failure may have been imbalances in the electrical field due to the improper alignment of the electrodes.
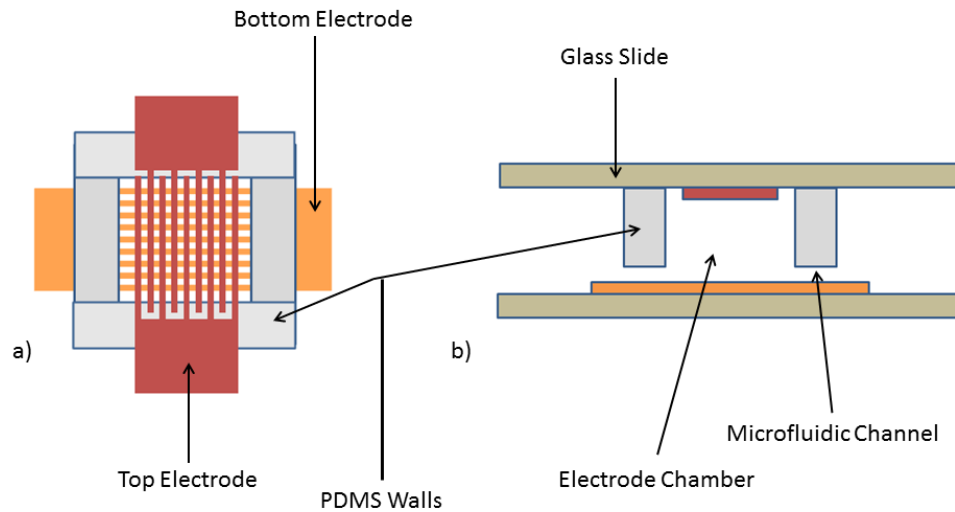
Figure 8: A concept drawing of the completed device with the PMDS in a) an overhead view and b) a side, cut-view showing the structures of the device that would

A detailed example of the proposed devices is shown Fig. 8. It uses the same design scheme as the prototype pictured in Fig. 7 because initial calculations showed that design to be most likely to function properly. An overhead and a cut-away view are provided to more clearly illustrate the construction he device's construction. This includes the incorporation of PDMS. As can been seen in Fig 8a&b, the PDMS forms stable walls between the two glass slides containing the electrode plates. In particular, Fig. 8b shows how the micro-fluidic channels lead into an electrode chamber. A simple syringe on an automated pump would be an easy means of injecting the cells along the channel towards the chamber.

III. Fabrication

The fabrication processes will be described in this section. Of note, this involved working with two different types of photoresist (Shipley S1813 and SU-8); the Shipley is a positive type of photoresist and the SU-8 is a negative form. Positive photoresists respond to UV radiation exposure by becoming much easier to remove via a chemical developer. Negative photoresists behave in an opposite fashion by exposed regions hardening and becoming much more resistant to developer; consequently the unexposed regions are removed leaving the mold shape intact. Both forms of photoresist were exposed in a mask aligner set for 2.5 J of UV radiation at a wavelength between 350-400 nm, but the times of exposure varied due to the chemical requirements of each kind of photoresist. Each had its own specific procedures for proper use and both processes will be described. The process for forming the electrodes will be described first and then the potential molds for the PDMS. Lastly, we will explain our PDMS development procedure.

Figure 9: Stations in the clean room facilities in Kaya Lab used during fabrication include a) the M-150 microscope/probe station where fabricated molds and electrodes were inspected and b) the mask aligner used for exposing the photoresists.

The Electrodes

The electrode components for the device were fabricated through a combination of metal deposition, photolithography and wet etching. This process began with the deposition of copper onto a standard glass microscope slide at a thickness of 91 nm. The deposition was carried out in the physics department on CMU's campus. The process normally takes several hours to complete. Once this was done, the actual shaping of the electrical components could be completed.

To shape the electrodes, the glass slide was first cut into three sections. It allowed for the possible yield of three electrode components from one slide. Photolithography techniques were applied to each section of glass slide. We applied Hexamethyldisilizane (HMDS) to all three portions and then spun them at 3000 rpm for 30 seconds. It served to prepare the slides for the photoresist. HMDS helps ensure the photoresist properly clings to the wafer during spinning. Shipley S1813 positive photoresist was then applied and spun for an additional 30 seconds at 3000 rpm. Once spinning was completed, the samples were each placed on a hot plate (373.15 Kelvin) for 90 seconds; the samples were then each allowed to cool to room temperature. After properly cooling, the glass slide sections were ready for exposure in the mask aligner.

The slide pieces were taken to the mask aligner within Kaya Lab's clean room shown in Fig. 9. They were each exposed to UV radiation for 4.5 seconds. After exposure was complete, they were all replaced on the hotplate for 3:30 minutes and then allowed to cool. Developer and etchant could finally be applied to produce the final electrode shapes.

Tetramethylammonium Hydroxide (TMAH) developed the photoresist. The developer solution consisted of 5mL of TMAH to 50mL de-ionized water (DIH_2O)—a ratio of 1/10. Each sample was immersed and swished in the solution for 2:20 minutes. During this stage of fabrication, we observed the features of the mask quickly became very clear as the rest of the photoresist dissolved. Mask features first appeared after approximately 1 minute. Each slide portion was thoroughly rinsed in DIH_2O and gently dried before the etching stage.

The etching was done with Sodium Persulfate ($Na_2S_2O_8$)--diluted in DIH_2O at a ratio of 4/1(water to etchant). The etchant solution was heated to 328.15 K and poured into a Petri dish to fill it half way. Each electrode was then immersed into the solution for approximately 20-30 seconds. The excess copper quickly dissolved revealing the final shape of the electrodes. Finally, they were rinsed with DI water, methyl alcohol, and acetone to remove any remaining etchant and photoresist. The $Na_2S_2O_8$ also proved useful for removing extraneous copper from the slides that could potentially cause the electrodes to short out. Fig. 10 shows the results of the electrodes after fabrication. As can be seen, samples 10a and 10b were successfully fabricated. Sample 10c was damaged by excessive contact with $Na_2S_2O_8$.
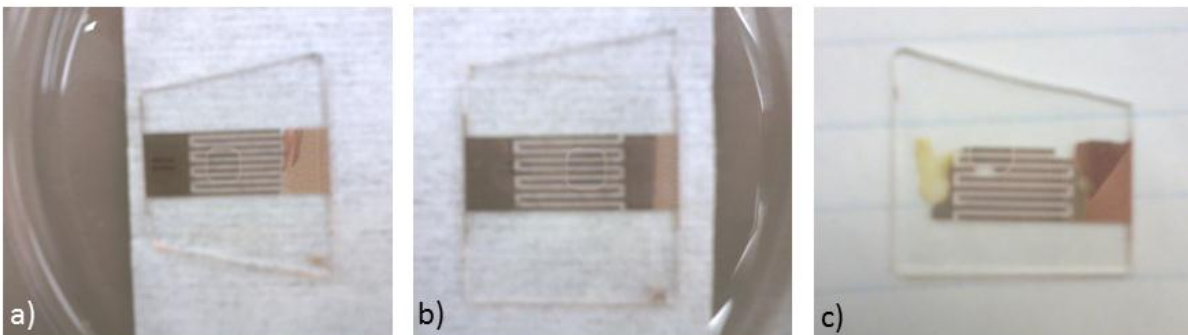

Figure 10: The three electrode samples after fabrication a-b) completed and intact, and c) destroyed during the etching process.

It was found that a simple matter of directing the DIH_2O bottle downward during an extra rinse was sufficient for protecting the integrity of the electrodes. The two intact samples were tested with a capacitance meter to verify their functionality. Their dimensions were 1.6cm by 0.8cm. The fingers 508μm in width and the spaces between them were also 508μm. Samples a) and b) passed with readings of 4.04pF and 4.06pF respectively.

SU-8 Mold Fabrication

SU-8 was the other form of photoresist we used during fabrication. SU-8's negative properties and higher viscosity made it ideal for constructing molds. A fair comparison between Shipley's S183 and SU-8 would be a thin, runny maple syrup to honey. Due to the thickness of the SU-8, HMDS wasn't needed to hold it in place. The development process was slightly different during this type of photoresist.

The SU-8 had to be properly prepared so that it could function as a suitable mold. Several mold designs were tried to refine this process. In theory, the PDMS could be properly shaped on the mold once this was accomplished. Before this could happen, however, the molds had to be suitably free from defects; two examples of defects we sought to minimize were trapped moisture and cracking in the developed SU-8. These could lead to the SU-8 being pulled off of the wafer after the PDMS cured.

SU-8 processing began by cleaning a 2-inch diameter silicon wafer with DI water and acetone. It was then centered on a spin-coater and the SU-8 was applied. A pipette was used to apply a sufficient amount of photoresist to the wafer. Due to its thick nature, the PDMS needed to be spread out with a spatula to ensure an even coating. Once evenly coated, the wafers were ready for spinning. This involved two spin cycles. The first cycle was 500 rpm for 5 seconds and the second was 3000 rpm for 30 seconds. After spinning was complete, the wafers underwent two hotplate treatments to prepare it for the mask-aligner. The samples were first placed on a hotplate set to 338.15 K for five minutes and then allowed to cool. Next, they were placed on a second hotplate set to 368.15 K for 20 minutes and then allowed to cool. We next exposed the wafers in the mask aligner, but UV exposure was done differently than the electrode processing.

The main difference in the exposure process was that two different exposure times were attempted to evaluate which may be more effective for future fabrications. These intervals were 10 seconds and 15 seconds. After the exposing the wafers, a "post bake" for 5 minutes at 338.15 K and then 15 minutes at 368.15 K prepared the molds for the chemical developer. The wafers were submerged and swished in the developer for 30 minutes and rinsed in DIH_2O and isopropyl alcohol. There was no cooling time after the post bake. The shapes of the molds became noticeable after several minutes of submersion in the SU-8 developer. After rinsing the wafers, a final hard bake at 425.15 K for 10 minutes helped to remove any remaining moisture and correct minor structural defects in the mold.

We prepared three separate batches of wafers to gain a better insight into which yielded the best results. Fig. 11 provides an image of all of the wafers that received SU-8 processing. The total processing time for two wafers was approximately 4 hours. This allowed sufficient time for all

the required heat, chemical and radiation treatments to be performed. It also provided sufficient time to record observations related to lab procedure and processing results.
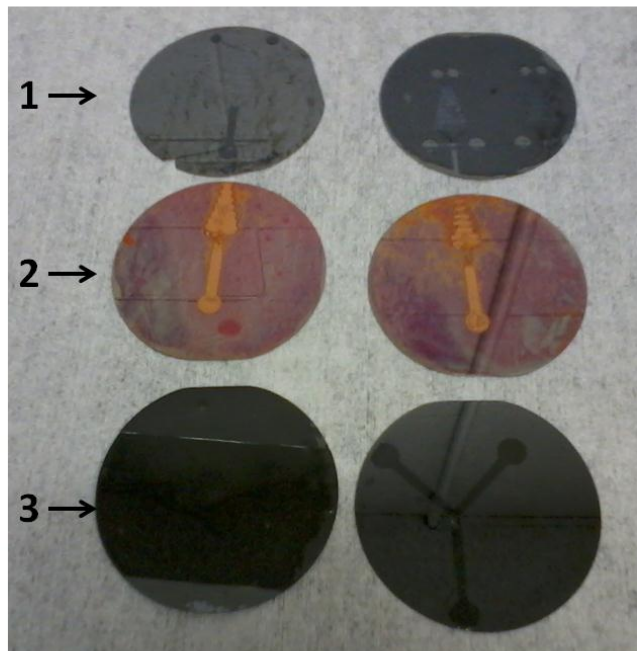

Figure 11: The six wafers that were processed up to the writing of this paper. They are numbered according to when they were fabricated—in chronological order.

The first two wafers were completed using a 15 and 10second UV exposure time in the mask aligner to see which worked better. This was effectively the trial run. A couple of other major differences with the first trial were that there was no hard bake done after processing and a mask for positive photoresist was used; this meant that shapes seen in the top two wafers were actually the sections dissolved by the developer. The rest of the SU-8 polymerized. Hard baking was suggested after the first fabrication attempt. The second and third sets of wafers were prepared with 10 seconds UV exposure and included a hard bake. The results of the processes will be discussed in the next section.

PDMS

Dow Corning Sylgard 182 Silicone met the requirements for our testing due to its quality and price. This PDMS performed well during an initial molding trial. That procedure will be described here.

Before the PDMS was mixed, the mold needed to be properly secured. Tape fastened the mold into a Petri dish. Aside from keeping the wafer firmly in place, this also served to seal the outer edges of the mold to prevent the silicone from getting under the wafer's edges. If this had happened, it would have put the mold at risk of severe damage. The actual PDMS preparation required little time or effort. The basic method for mixing this type of silicone was a 10/1 ratio of PDMS to curing agent. For trial described here, 11 grams of PDMS was mixed with 1.1 grams of curing agent and mixed to proper consistency. After mixing and pouring onto the mold, a standard technique is to place the PDMS in a vacuum chamber to remove excess air bubbles. As we lacked this equipment, we placed the PDMS in the fume hood and allowed it to sit over night. Surprisingly, most of the air bubbles disappeared by the next day. The PDMS had a tacky, sticky quality to it. To remedy this, the PDMS was cured on a hot plat at 313.15 K for 1 hour. This removed the sticky feel to the silicone and left it with a firm, rubbery feel as can be seen in Fig. 12a.
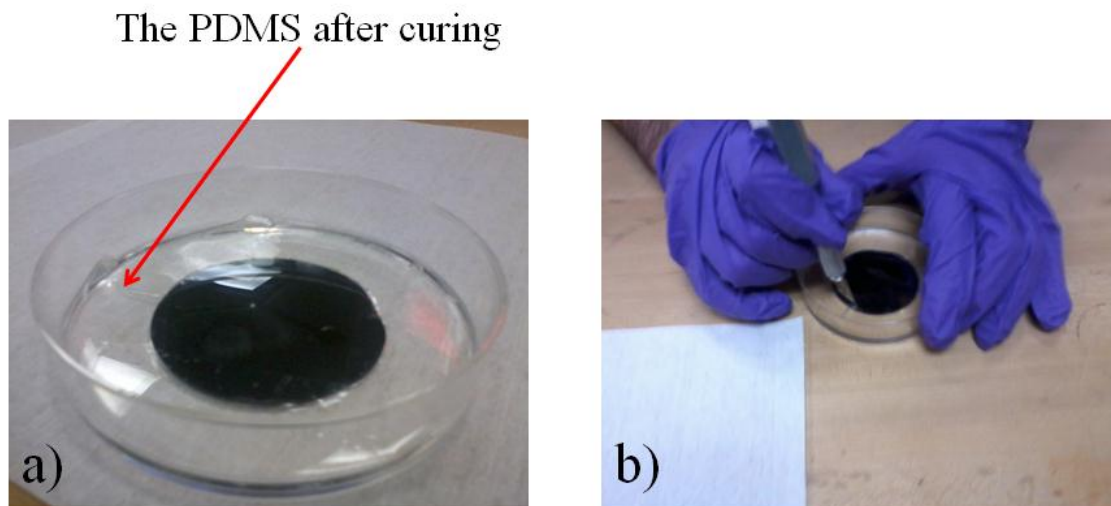

Figure 12: The PDMS a) after curing was completed and b) as the microfluidic structure is being removed from the mold.

Fig 12b is a picture of the separation process of the PDMS structure from the mold. Removing the shaped PDMS only required carefully cutting around the structures to easily separate the two. This also demonstrates another benefit of using silicon wafers as substrates for SU-8 molds: the silicon is very difficult to scratch, requiring a diamond to do so. This offered the freedom to cut with a fair degree of pressure around the mold. In Fig. 13, the final microfluidic structure and the remaining PDMS are revealed.
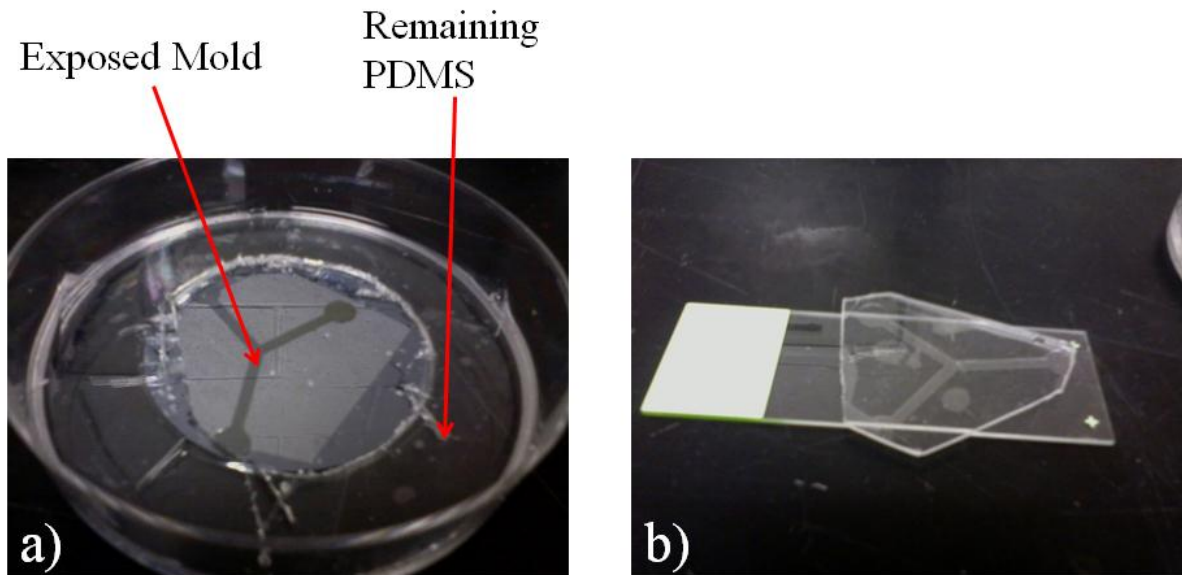
Figure 13: The results a) of the underlying mold after removing the PDMS and b) the finished microfluidic structure.

Future microfluidic channels will be at the scale of approximately 50μm by 100μm by 1cm. They will be the same basic shape as demonstrated in Fig. 13b. Such fabricated structures will be ideal for the observation of fluid and cellular behavior, but this test yield successful results and indicated promise for future fabrications.

III. Results

As the details and results for the electrodes have been already discussed earlier in the paper, the majority of the results discussed here shall pertain to the SU-8 molds. The PDMS shaping will also be mentioned. It will be noted, that the electrode fabrication appeared to yield encouraging results as it produced two complete and functional electrical components. The wafers used for SU-8 fabrication yielded their own results that served as a means to better learn and refine the process over three steps.

One major observation during fabrication was the difference in UV exposure times. It was decided to try a 15 second exposure on one wafer and a 10 second exposure on the second. This happened during the first wafer batch to evaluate which more effectively developed the photoresist. Inspections of both wafers with normal, visual means and with a microscope revealed that 15 seconds over-developed the SU-8 rendering it unsuitable. A 10 second exposure interval consistently demonstrated better results for the remaining SU-8 processes.
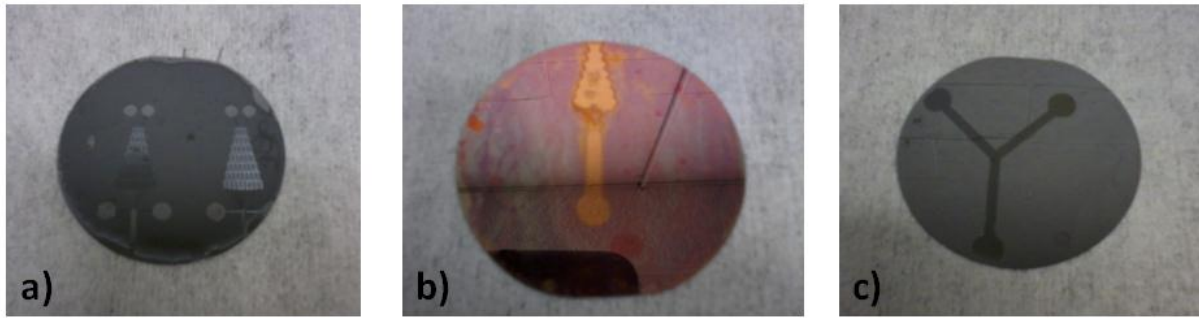
Figure 14: Closer views of the wafers from a) the first trial, b) the second trial, and c) the third trial.

Fig. 14 provides a closer view of wafers from each fabrication. Images a & b from Fig. 14 reflect slightly more complex masks for possible molds. We wanted to focus on refining the consistent accuracy of the SU-8 procedure at this stage. Of the first two batches, the wafer shown in 14a offered clearer detail than wafer 14b. In part this could be due to the fact that the micro-fluidic shapes were where the photoresist was actually removed (as in "hollowed out"). In the second case (14b) the only SU-8 remaining on the wafer is the mold shape. The reddish discoloration on the wafers from the second batch (Fig 11 and 14b) stemmed from the silicon and oxygen the surface of the wafer effectively forming silicon oxide (SiO); this is a fairly common occurrence for silicon wafers. Fig. 14c provides an image of the most recent mold. The main aim of the third mold was simplicity. The basic "y-shape" offered simpler system of channels which better suited our purposes at this time. Less complication also meant a greater likelihood of the PMDS structures correctly forming. Notice in Fig. 14c that at the end of each arm there is a rounded cap. Each cap will serve as a reservoir where sample materials can be both introduced into the channels and pooled together after mixing. Different materials would be introduced into two of the three arms and ideally they should interact in the third channel. A closer example of some of the microscopic structures created during fabrication can be seen in Fig. 15.
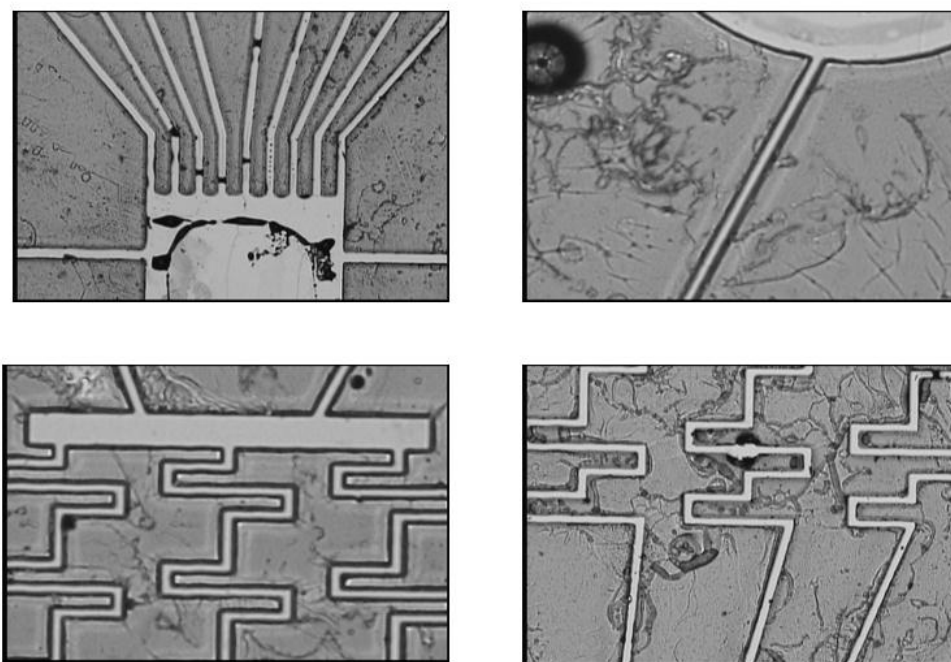
Figure 15: Several images captured from the first wafers produced.

The images in Fig. 15 were taken from the first batch of molds. Of the three sets, these two offered the most filmable visual data. The various complex patterns created in the polymerized SU-8. Effectively, microchannels have been created in the photoresist itself. With time, this may prove to have useful applications in itself. If PDMS were applied to this type of mold, however, microchannels wouldn't be created but rather a rigid structure that bore their inverted shape. Another possibility would be that SU-8 could be damaged upon removal of the PDMS. This was also why a simpler shape was chosen for the initial experimentation to be carried out with the PDMS. Examinations of the sample revealed that it offered greater stability for the needs of the initial PDMS testing.

The simple shape of the SU-8 mold appeared to be the correct choice when PDMS was actually applied to it. The PDMS channels reflected excellent detail and the SU-8 mold maintained its integrity during separation from the PDMS. This offered the opportunity to create further microfluidic structures on that same wafer. It also suggested that reducing the size of the y-shape structure down to the micrometer scale has a good chance of success. One possible pitfall might be that the SU-8 might not demonstrate the same resiliency during separation from the PDMS. This will require further experimentation, however, to evaluate the integrity of SU-8 at a smaller scale.

IV. Conclusion

The prospect of giving physicians a quick means of detecting serious illness is being explored by many researchers currently. The concepts offered in this paper are just one avenue towards that end. The literature and theoretical projections seem to suggest that the design proposed in this paper offers promise. The results from fabrication of the electrode components, the SU-8, and the PDMS structures are encouraging. The initial trials yielded products that appear to be relatively functional on their own. The next likely stage of testing will be reducing the size of the SU-8 molds to see how they perform with the PDMS at that scale of size. From there, work with using microfluidic channels to manipulate fluids and microbeads can begin of the microchannels produced provide good structural integrity.

As the basic means to assemble a device seem available, it is likely that another prototype of a device will be constructed and tested in the near future. The first device will use tape to separate the top and bottom electrodes and later models will incorporate the PDMS. Mainly, the first goal is to get a single microbead to rotate in the e-field. Once that is accomplished, this research can branch out into work with living cells It is also possible that the design of the electrode structures will change due to further data gathered from testing. This will only serve to hopefully provide a much more effective design.

During the course of this research, it has opened opportunities for cross-discipline learning and communication between individuals of different academic backgrounds. Chemistry, biology, physics, and electrical engineering approaches have all been involved with the various stages of this project. The research required to prepare for this type of work was also key to improving the understanding needed to participate and invaluable for adding to a student's knowledge acquired from course work. Yet, it allows an experimental setting for students to apply and develop their learning further. The over-all goal is to not only contribute to this field of research but to engineering education as a whole.

Acknowledgements

Bibliography

[1] C. Dalton, S. Adamia and L. M. P. a. K. V. I. S. K. , "Investigation of human malignant cells by electrorotation," in *2004 Annual Report Conference on Electrical Insulation and Dielectric Phenomena*, 2004.

[2] C. Chuang, C. Li, C. Yeh and a. Y. Hsu, "Electrorotation of HL-60 Cells Uptake of Metal and Dielectric Nanoparticles in a Stationary AC Electric Field," in *Proceedings of the 3rd IEEE Int. Conf. on Nano/Micro Engineered and Molecular Systems* , Sanya, China, 2008.

[3] R. Elbez, B. H. McNaughton, L. Patel, K. J. Pienta and a. R. Kopelman, "Nanoparticle Induced Cell Magneto-Rotation: Monitoring Morphology, Stress and Drug Sensitivity of a Suspended Single Cancer Cell," *PLos ONE,* vol. 6, no. 12, pp. 1-11, 2011.

[4] Q. Hu, R. P. Joshi and a. A. Beskok, "Model study of electroporation effects on the dielectrophoretic response of spheroidal cells," *JOURNAL OF APPLIED PHYSICS,* vol. 106, pp. 1-8, 2009.

[5] P. Wanichapichart, T. Wongluksanapan and a. L. Khooburat, "Electrorotation: Diagnostic Tool for Abnormality of Marine Phytoplankton Cells," in *Proceedings of the 2nd IEEE International Conference on Nano/Micro Engineered and Molecular Systems*, Bangkok, Thailand, 2007.

[6] C. Huang, Y. Wu, L. Wang and a. J. Yu, "Negative Dielectrophoretic Force Assisted Determination Differences between Autotrophic and Heterotrophic Algal Cells Using Electrorotation Chip," in *Proceedings of the 1st IEEE International Conference on Nano/Micro Engineered and Molecular Systems*, Zuhai, China, 2006.

[7] H. Li, D. Chen and a. Q. Yang, "Image Processing Technique for Characteristic Test of Cell Based on Electrorotation Chip," IEEE, Hangzhou ,Zhejiang Province, China, 2008.

[8] Qihua, L. G. L. Hao and a. L. Yanling, "Cell Electrorotation Motion Parameters Detection Based on Image Processing," in *2009 World Congress on Computer Science and Information Engineering*, 2009.

[9] H. Zhang, X. Liui, X. Shao, X. Wang and a. B. Zhou, "The study of the improved wavelet thresholding with translation invariant de-noising on capillary electrophoresis signal," in *Proceedings of the 2009 4th IEEE International Conference on Nano/Micro Engineered and Molecular Systems*, Shenzhen, China, 2009.

[10] M. Behnam, G. Kaigala, M. Khorasani, S. Martel, D. Elliott and a. C. Backhouse, "Integrated circuit-based instrumentation for microchip capillary electrophoresis," *IET Nanobiotechnol,* vol. 4, no. 3, pp. 91-101, 2009.

[11] T. Kikuchi, T. Ujiie, T. Ichiki and a. Y. Horiike, "Fabrication of Quartz Micro-Capillary Electrophoresis Chips for Health Care Devices," in *Microprocesses and Nanotechnology Conference, 1999. Digest of Papers. Microprocesses and Nanotechnology '99. 1999 International*, 1999.

[12] H. Liao, Y. Liao, J. Yi and a. Y. Huang, "Study of orthogonal vector lock-in amplifier in contactless conductivity detector of electrophoresis microchip," in *201O International Conference on Computer Application and System Modeling (ICCASM 2010)*, 2010.

[13] O. Montero, R. Ibarra and a. R. Garcia, "POWER SUPPLY FOR ELECTROPHORESIS PROCESS," *Industrial Electronics, Control, and Instrumentation, 1995., Proceedings of the 1995 IEEE IECON 21st International Conference,* vol. 1, pp. 568-571, 1995.

[14] E. Zacharia, E. Kostopoulou, D. Maroulis and a. S. Kossida, "A Spot Segmentation Approach for 2D Gel Electrophoresis Images Based on 2D Histograms," in *2010 International Conference on Pattern Recognition*, Athens, Greece, 2010.

[15] S. Kim, S. Zhou, Y. Hu, M. Acik, Y. J. C. C. Berger, W. d. Heer, A. Bongiorno and a. E. Riedo, "Room-temperature metastability of multilayer graphene oxide films," *nature Materials,* vol. 11, pp. 544-549, 2012.

[16] K. P. Loh, Q. Bao, G. Eda and a. M. Chhowalla, "Graphene oxide as a chemically tunable platform for optical applications," *nature Chemistry,* vol. 2, pp. 1015-1024, 2010.

[17] X. Zhu, H. Yi and a. Z. Ni, "Novel Design of Multiphase Optoelectronic Microfluidic Device for Dielectric Characterization of Single Biological or Colloidal Particles," IEEE, 2009.

[18] M. Krogh, "Soft Lithography for Dummies: A Reference for The Rest of Us!," Linkoning University, 2009.

[19] A. C. M Renno, P. A. McDonnell, M. C. Crovace, E. D. Zanotto, L. Laakso, "Effect of 830 nm Laser Phototherapy on Osteoblasts Grown In Vitro on Biosilicate® Scaffolds," *Photomedicine and Laser Surgery* , vol. 2, no. 1, pp. 131-133, 2010.